

## The Physical Properties and Morphology of Poly- $\epsilon$ -caprolactone Polymer Blends

DOUGLAS S. HUBBELL and STUART L. COOPER, *Department of Chemical Engineering, University of Wisconsin, Madison, Wisconsin 53706*

### Synopsis

The compatibility, morphology, and mechanical properties of poly- $\epsilon$ -caprolactone (PCL) blended with poly(vinyl chloride), nitrocellulose, and cellulose acetate butyrate are described in this study. Methods used in this investigation included differential scanning calorimetry, dynamic mechanical testing, small-angle light scattering, light microscopy and stress-strain testing. Blends of PCL with poly(vinyl chloride) (PVC) are shown to be compatible in all proportions. In the PCL concentration range 40–100%, the PCL crystallizes in the form of negative spherulites. The spherulites were found to be volume filling with as much as 35% PVC. The nitrocellulose blends with PCL exhibited the glass transition behavior of a compatible system over the composition range of 50–100% PCL. At lower PCL concentrations, phase separation was apparent. The PCL crystallinity was present only in the nitrocellulose blends with more than 50% PCL, and it was in the form of rod-like superstructures. Blends of PCL with cellulose acetate butyrate were shown to be phase separated, with one phase having nearly equal proportions of the two polymers. The PCL crystallinity was in the form of negative spherulites and was formed with PCL compositions as low as 50%. Stress-strain results show polycaprolactone to be an effective plasticizer for poly(vinyl chloride) and the cellulose derivatives studied.

### INTRODUCTION

A polymer blend is a mixture of two or more different kinds of polymer chains which are not covalently bonded together. This separates blends from block or graft copolymers in which primary bonds link dissimilar chain segments. Compatibility is a relative term used to denote the degree of mixing in a solution, be it for small molecule liquids or for polymer solids. The lack of compatibility between substances leads to phase separation. In blends, macroscale phase separation can lead to a material with very poor mechanical properties due to the presence of large domains which have poor interfacial bonding.

In contrast, a compatible blend exhibits a high degree of mixing and mechanical properties which reflect an average between the constituent polymers. For example, plasticized blends of poly(vinyl chloride)/nitrile rubber combine the low-temperature flexibility and ease of processing of nitrile rubber and the high-temperature permanence and flame retardant properties of poly(vinyl chloride). Another example is blends of poly(phenylene oxide) with styrene copolymers. These blends have the excellent dimensional stability at high temperatures and good electrical properties of poly(phenylene oxide) combined with the lower melt viscosity, shear sensitivity, and cost of polystyrene.<sup>1,2</sup>

Although highly incompatible mixtures of polymers are easy to detect because of their opacity and poor mechanical properties relative to the constituent polymers, complete compatibility is less easily demonstrated. If domains are present, they can often be seen with light or electron microscopes. Completely incompatible polymer films are often opaque, but compatibility is a relative term, and domains may be quite small, resulting in an optically clear specimen. In addition, the index of refraction of the different phases may be similar and allow an incompatible film to be completely clear. Another difficulty is that often the images seen by microscopy are not easily interpreted.

Compatibility may be studied by mutual solvent and light-scattering techniques, which are based on thermodynamic considerations.<sup>3</sup> Moreover, the various methods of determining the glass transition ( $T_g$ ) of a polymeric material can be applied to blend systems. Normally, compatible systems will exhibit only one  $T_g$  located between the  $T_g$ 's of the constituent polymers. In contrast, an incompatible blend will show the  $T_g$ 's of the homopolymers. It is now generally accepted that a single intermediate  $T_g$  is proof of compatibility even though the sensitivity of the technique may vary. The glass transition can be measured by a variety of methods including thermal analysis, dynamic mechanical testing, changes in refractive index,<sup>4</sup> changes in specific volume on thermal expansion,<sup>5</sup> NMR,<sup>6</sup> and possibly gas chromatography,<sup>7</sup> though it has yet to be used for finding the  $T_g$ 's in a polymer blend.

## BLEND OF POLYCAPROLACTONE

Koleske and co-workers<sup>8</sup> have blended PCL, and many similar polyesters, with a wide range of polymers and have demonstrated many advantages of the blends over the homopolymers. Their blend systems may be divided into three categories. First, there are blends which have crystalline interactions between the two polymers. For example, a 90/10 blend of polyethylene and PCL exhibits an unaltered glass transition of the polyethylene, which would indicate a thermodynamically incompatible amorphous phase; but the crystalline relaxation maximum for polyethylene occurs at a higher temperature and has a higher magnitude. This phenomenon implies that the PCL restricts the motion of the crystalline polyethylene through some form of interaction.

A second classification of useful blends are those which exhibit the glass transitions of the constituent homopolymers and lack crystalline interactions but still have good mechanical properties. These are said to be mechanically compatible.<sup>9</sup> This behavior indicates that there is some connection between phases, and they differ from compatible systems, which exhibit a single  $T_g$ , only in the size of the domains and the extent of the phase separation. Examples of polymers which form mechanically compatible blends with PCL are poly(vinyl acetate), polystyrene, poly(methyl methacrylate),<sup>9</sup> and poly( $\epsilon$ -methyl- $\epsilon$ -caprolactone).<sup>10</sup>

The third classification are blends which exhibit only one  $T_g$  which is intermediate to those of the constituent homopolymers. Polymers that can be blended compatibly with PCL include poly(vinyl chloride), nitrocellulose, phenoxy A (a poly(hydroxy ether) made by Union Carbide), Penton (a chlorinated polyether), styrene-acrylonitrile copolymers, and polyepichlorhydrin.<sup>9</sup>

### Blends of Poly- $\epsilon$ -caprolactone and Poly(vinyl Chloride)

Koleske and Lundberg<sup>11</sup> found that PCL/PVC blends were compatible over the full range of compositions. Each blend in the range 10%–90% PVC exhibited only one  $T_g$ . Furthermore, it was found that the  $T_g$  versus weight fraction plot could be represented quite well by two  $T_g$  copolymer equations, the Fox equation,<sup>12</sup>

$$(1/T_{g12}) = (W_1/T_{g1}) + (W_2/T_{g2}) \quad (1)$$

and the Gordon–Taylor equation,<sup>13</sup>

$$T_{g12} = T_{g1} + [k W_2(T_{g2} - T_{g1})W_1] \quad (2)$$

where  $T_{g12}$  is the glass transition of the copolymer or blend,  $T_{g1}$  and  $T_{g2}$  are the glass transitions for homopolymers 1 and 2,  $W_1$  and  $W_2$  are weight fractions, and  $k$  is a constant.

They found that the loss modulus ( $G''$ ) peaks, which represented the  $T_g$ 's for the blends, when extrapolated to 100% PCL gave a  $T_g$  of 202°K even though the quenched  $T_g$  for the pure PCL samples was 213°K. This discrepancy was attributed to the influence of crystallinity on the  $T_g$  of the PCL homopolymer.

The PCL/PVC blend system was next studied by Ong.<sup>14</sup> All samples were cast from methyl ethyl ketone solutions by evaporating the solvent at room temperature. Ong found that crystallinity was present in blends with up to 70% PVC by weight. The crystallinity had a spherulitic superstructure in all cases, and the spherulites were volume filling with less than 50% PVC. The lamellae, which were investigated by optical and electron microscopy, were found to twist regularly in the blends as they radiated from the centers of the spherulites. In contrast, the pure PCL was found to have irregular twisting of the lamellae. Although the crystallite dimensions were found by x-ray diffraction to decrease with increasing concentrations of PVC, the unit cell dimensions were found not to change with the presence of PVC. Consequently, it was suggested that the PVC molecules were restricted to the interlamellar regions.

Further work on this system was carried out by Khambatta and Stein.<sup>15,16</sup> Their blend samples were cast in dishes at room temperature from solutions of tetrahydrofuran (THF), heated to 70°C, and then slowly cooled. With this sample preparation, samples exhibited somewhat less crystallinity (60% for PCL) than the samples prepared by Ong. As a result of small-angle x-ray scattering (SAXS), they concluded that the amorphous regions in all the blends consisted of two phases. Each phase contained both polymers but in different proportions, and there appeared to be a transition zone between the phases which was about 30 Å thick. The crystalline structure was investigated both by SAXS and small-angle light scattering. They confirmed Ong's findings that the crystallinity was spherulitic and that the spherulites, which become coarser with increasing amounts of PVC, were volume filling until nearly 50% PVC. They postulated that the PCL could not crystallize in high concentrations of PVC because the domain size for the PCL-rich phase became smaller than the size of a critical nucleus.

### Blends of Poly- $\epsilon$ -caprolactone and Cellulose Derivatives

Cellulosic derivatives are generally too stiff to be processed without some sort of plasticizer.<sup>17</sup> Since few small molecule plasticizers seem to be effective because

of migration and volatilization, polymer blending is potentially quite important to the use of these thermoplastics, especially since polymeric plasticizers migrate very slowly.

Brode and Koleske<sup>9</sup> cast samples of nitrocellulose (NC) (12% nitrogen) blended with PCL from a solvent mixture of isopropanol and *n*-propyl acetate. As with the PVC/PCL system, they heated the samples above the  $T_m$  of PCL and quenched them in liquid nitrogen before proceeding with torsion pendulum experiments. The  $T_g$  as indicated by both  $Q^{-1}$  and  $G''$  increased steadily with increasing concentrations of NC for the 0–50% NC range.

Stress-strain measurements reveal that the modulus drops and the ability to elongate increases with increasing amount of PCL. Thus, PCL acts as an excellent plasticizer for nitrocellulose. Also, diluting the nitrocellulose with PCL would most likely increase the stability of nitrocellulose to sunlight and heat and thus counteract the main limitations of the material.

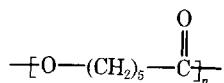
Koleske, Whitworth, and Lundberg<sup>8</sup> also blended PCL by various methods with acetylated ethyl cellulose, carboxymethyl cellulose, triacetate cellulose, diacetate cellulose, and cellulose acetate butyrate and found that each cellulosic could form mechanically compatible blends with PCL. For the most part, the PCL proved an effective plasticizer which gave cellulosic blends that were easier to process and more flexible than the pure cellulose esters and ethers.

The objectives of the present study were to analyze polymer blends of poly- $\epsilon$ -caprolactone with poly(vinyl chloride) and with several cellulose derivatives. The research included the determination of compatibility and the characterization of the morphologic, mechanical, and orientation properties of the poly-caprolactone blends. The use of differential infrared dichroism for following the dynamic orientation of each component of the compatible amorphous and semicrystalline blends will be reported elsewhere.<sup>18</sup>

## EXPERIMENTAL

### Materials

The polymer common to all binary blend systems studied here is poly- $\epsilon$ -caprolactone (PCL), which has the repeat unit



The PCL used in this study was supplied by Dr. J. V. Koleske of Union Carbide Corporation's Chemicals and Plastics Division and was designated as PCL-700. Other studies on the poly- $\epsilon$ -caprolactone–poly(vinyl chloride) blend system have also used PCL-700.<sup>11,14,16,19</sup> The PCL had been solution polymerized and was in the form of extruded yellow pellets. It is a semicrystalline polymer with a melting point of 61°C.

The polymers blended with PCL were cellulose acetate butyrate, nitrocellulose, and poly(vinyl chloride). All blends are designated in terms of the weight per cent of polymer mixed with PCL. The cellulose acetate butyrate (CAB) had 1.7 butyl and 1.0 acetyl groups per repeat unit and was designated 381-20 by the manufacturer (Tennessee Eastman Company). Although the white CAB powder

supplied showed a small amount of crystallinity melting at 168°C, films made from the powder failed to show any sign of a crystalline melting point using differential scanning calorimetry. The nitrocellulose used (supplied by Hercules, Inc.) was designated RS 1/2 sec. It was furnished as a white powder packed with isopropyl alcohol (30% by weight) because of its flammability. It is reported to be 11.8–12.2% nitrogen, which corresponds to  $2.25 \pm 0.06$  nitro groups per glucose ring. The poly(vinyl chloride) (PVC) used was Union Carbide's QYTQ-387 which was supplied by Koleske and had been used in several other PCL/PVC studies.<sup>11,14,16,43</sup>

Films made of pure CAB, NC, and PVC were all clear. The lack of crystallinity in CAB could be confirmed by thermal analysis, but both PVC and NC degraded below their expected melting points. The NC was assumed to be mostly amorphous. The PVC crystallinity has been estimated to be less than 8% by comparing carbon–chlorine stretching bands in the infrared spectrum.<sup>14</sup> The molecular weights, densities, and solubility parameters for PCL, CAB, NC, and PVC appear in Table I. The solubility parameters have been calculated by the group contribution methods of Small<sup>21</sup> and Hoy.<sup>22</sup>

### Sample Preparation

All samples for this study were prepared by spin casting from polymer solutions. In this technique, which has been described elsewhere,<sup>23</sup> a solution of polymers and solvent is forced against the walls of a spinning cylinder. The solvent is evaporated by a slight vacuum and also by heat if desired, with the polymer precipitating onto a sheet of aluminum or paper lining the wall. With this technique, it has been demonstrated that unoriented films with thicknesses as small as 4  $\mu$  can be made.

Tetrahydrofuran (THF), which has a solubility parameter of 9.1, was used as the spin-casting solvent. In all sample preparations, the solutions were cast at room temperature. Films for IR work were precipitated from approximately 15 ml of 1% solution; and for samples thicker than 10  $\mu$ , portions of 5% solution were added every 15 min to the caster. All samples were dried in a constant stream of air for several hours and then dried for at least four days under vacuum at room temperature. Films thicker than 25  $\mu$  were dried for at least one week. After drying, all samples were aged in desiccators at room temperature for at least two weeks. This allows the PCL crystallinity to approach its equilibrium value.<sup>11</sup>

TABLE I  
Characterization of Polymers Used

	PCL	PVC	CAB	NC
$\bar{M}_n$	13,000	35,000	77,000	45,000
$\bar{M}_w$	24,000	72,000	—	—
Repeat unit molecular weight	114.145	62.499	323.3	262.6
Density, g/cm <sup>3</sup> (20°C)	1.149	1.39	1.15–1.22	1.58–1.65
Solubility parameter—Hoy, <sup>22</sup> (cal/cm <sup>3</sup> ) <sup>1/2</sup>	9.43	9.47	9.57	9.95
Solubility Parameter—Small, <sup>21</sup> (cal/cm <sup>3</sup> ) <sup>1/2</sup>	9.34	9.55	8.90	—

<sup>a</sup> The densities for the amorphous and crystalline PCL are 1.094<sup>44</sup> and 1.187<sup>14</sup>, respectively.

The only exception to the above procedure was with some of the samples containing PVC. It was found that in samples dried at room temperature, the glass transitions were depressed somewhat. The amount of depression of the  $T_g$  depended on the per cent PVC and the thickness of the film. In pure PVC samples, the  $T_g$  was depressed as much as 51°C for a 360- $\mu$  sample or as little as 8°C for a 8- $\mu$  film. This retention of solvent even at processing temperatures and its effect on PVC properties is well documented.<sup>24,25</sup>

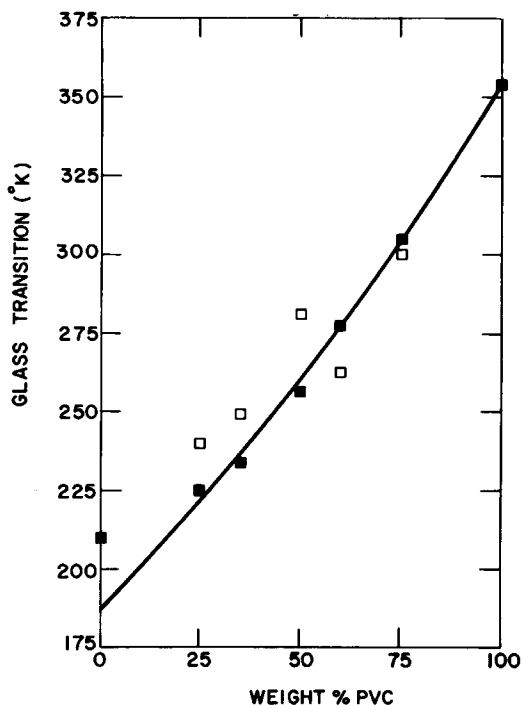


Fig. 1.  $T_g$  vs weight percent for (□) PVC/PCL with the Gordon-Taylor equation fit to the (■) quenched data.

It was found that temperatures greater than 80°C were needed to remove the solvent from the PVC samples. Therefore, samples of PVC, PVC blends, and PCL were prepared with 1% Ferro GH-148 liquid thermostabilizer based on the total weight of polymer (Ferro Corporation). These samples were approximately 70  $\mu$  thick and were dried under vacuum for 48 hr at room temperature, 48 hr at 105°C, and finally for an additional 60 hr at 48°C. The final drying period was used to help restore the crystallinity lost by melting. These particular samples were annealed at room temperature for an additional two weeks before being used in the DSC and stress-strain measurements. The PVC and 75% PVC samples were somewhat yellowed, but the other samples seemed unaffected in appearance. The dryness of PVC film was confirmed by a DSC measurement of the  $T_g$ . For all other experiments, the thin and delicate samples were only dried at room temperature. The amount of solvent in these thin samples was small enough to not seriously affect the results.

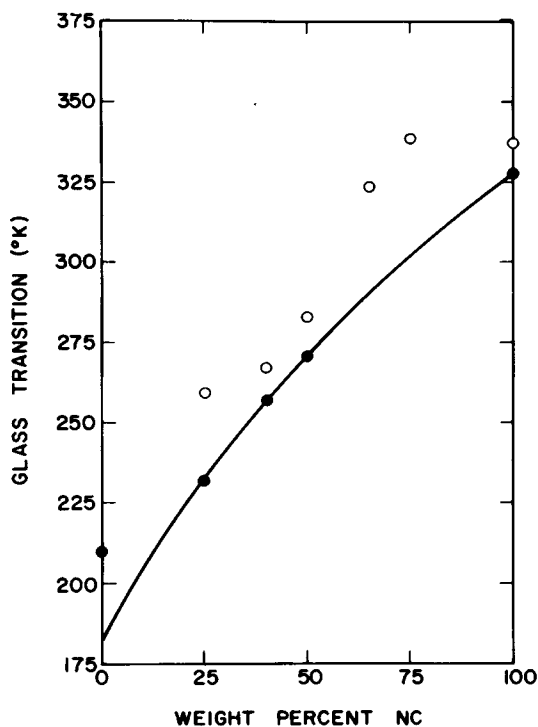


Fig. 2.  $T_g$  vs weight percent for (O) NC/PCL with the Gordon-Taylor equation fit to the (●) quenched data.

### Mechanical Properties

Mechanical properties of the blend systems were determined by two tensile methods. The first was dynamic mechanical testing at a constant frequency over a wide temperature range. This experiment yields information on dynamic modulus and molecular relaxation processes. Secondly, standard tensile stress-strain tests were performed to measure the modulus, ultimate strength, and elongation at break.

The dynamic elastic modulus  $E'$ , the loss modulus  $E''$ , and the  $\tan \delta$  were measured simultaneously by the Rheovibron dynamic viscoelastomer Model DDV-II (Toyo Measuring Instruments Co., Ltd.). Measurements were made at a frequency of 110 Hz starting from  $-140^\circ\text{C}$  and heating at  $1^\circ\text{--}2^\circ\text{C}$  per minute until the samples became too soft to be tested. The readings were taken every  $4^\circ\text{--}8^\circ\text{C}$  except in transition zones, when the readings were taken every  $2^\circ\text{C}$ . The sample chamber was kept dry by a stream of moisture-free nitrogen.

Standard tensile stress-strain experiments were performed at room temperature on an Instron table-model testing machine. All samples were die cut from spin-cast films into standard dumbbell shape (ASTM 412 Type D) with a gauge length of 2.0 in. and a width of 0.126 in. The elongation rate was 0.2 in./min, which is an engineering strain rate of 10%/min. The sample thickness, which was measured with a micrometer, varied from blend to blend ( $70\text{--}100\ \mu$ ) because samples were made on the basis of weight and not density. The PVC blended films were made somewhat thinner ( $50\text{--}70\ \mu$ ) to facilitate drying. All reported results are the average of three to four runs.

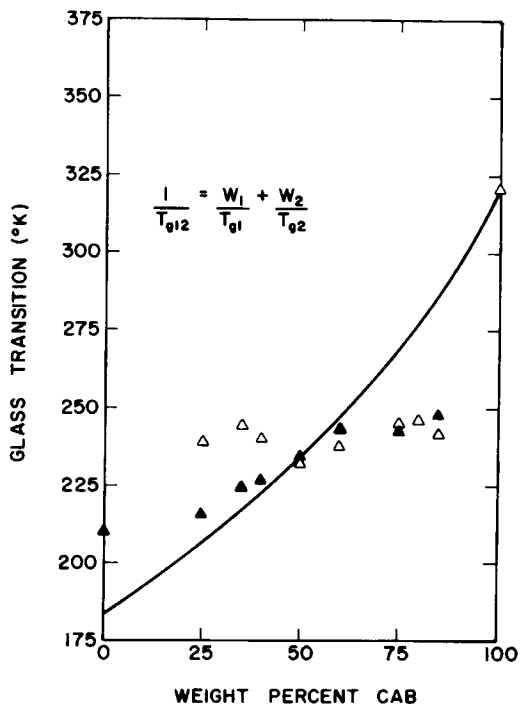


Fig. 3.  $T_g$  vs weight percent for (△) CAB/PCL with the Fox equation fit to the (▲) quenched data.

### Thermal Studies

Differential scanning calorimetry (DSC) was used to measure heat capacity as a function of temperature. The DSC used in this study was a Perkin-Elmer Model DSC-2. Liquid nitrogen was used as a heat sink, and helium was used as the purge gas. Samples were usually about 30 mg, and a heating rate of 20°/min was used for measuring  $T_g$  and  $T_m$ . For measuring heats of fusion, the heating rate was 2.5°/min. The heat of fusion peak areas were always greater than 10 in.<sup>2</sup> and were measured with a planimeter. The percent crystallinity was calculated on the basis of a heat of fusion of 32.4 cal/g for PCL, which was found by melting point depression experiments for PCL using ethyl benzoate as diluent.<sup>26</sup> The reference for the heat of fusion calculations was pure indium, which melts with a heat of fusion of 6.80 cal/g.

### Morphology Studies

For a complete description of the morphology of a polymer sample, several techniques must be employed because of the different levels of crystalline structure and the limitation of each method. In this research, optical microscopy and small-angle light-scattering were employed to study blend morphology. The small-angle light-scattering apparatus used in this work was a Spectra Physics Model 115 He-Ne continuous-wave gas laser emitting a polarized light beam with a wavelength of 6328 Å. The beam passes through the sample and then through



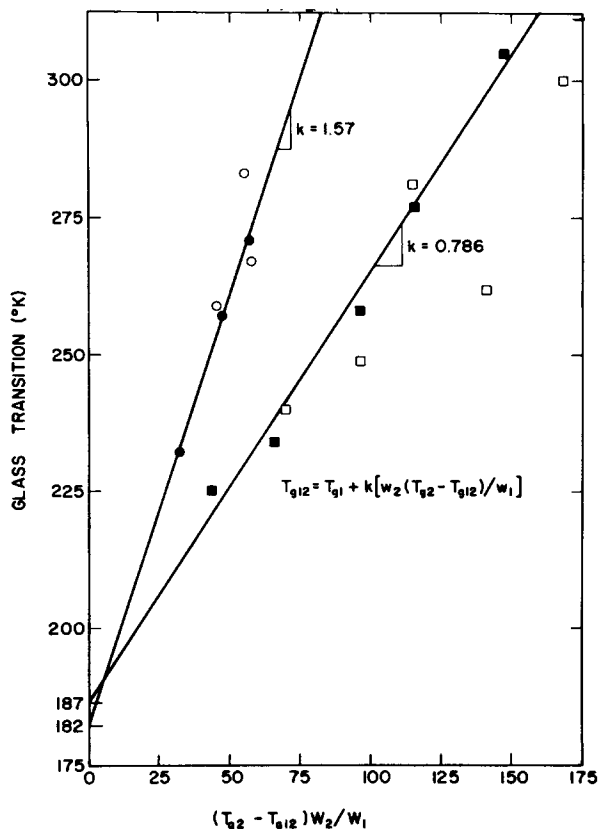


Fig. 4.  $T_g$  data for (■) PVC/PCL and (●) NC/PCL blends plotted according to the Gordon-Taylor equation. The lines are fit to the quenched data: (○) NC/PCL; (□) PVC/PCL.

an analyzer, which is a second polarizer. The resulting scattering pattern was recorded on Polaroid Type 52 black and white film. The samples used were approximately  $30 \mu$  thick, and the beam intensity was controlled by Wratten gelatine neutral density filters.

The refractive index within a sample can change due to presence of crystalline and amorphous regions, voids, changing anisotropy, and areas of different orientation. The first two are due to density differences, and the last two are due to orientation differences.<sup>14</sup> SALS was used in this study to determine the nature of the crystalline superstructure and to measure the average radius of the spherulites.<sup>27-30</sup>

All of the optical microscopy was conducted on a Zeiss Universal microscope. Pictures were taken with a 35-mm camera with Ektachrome color film for tungsten lamps. The samples were  $5-15 \mu$  thick and were held between glass slides. No heat treatment was used on the samples. The presence of spherulites was indicated by the usual Maltese cross extinction pattern which appears when using crossed polarizers. The sign of spherulites was found by inserting a quartz accessory plate in the path of the light. The extent to which the spherulitic superstructure filled the available volume was qualitatively determined along with the approximate size of the spherulites.

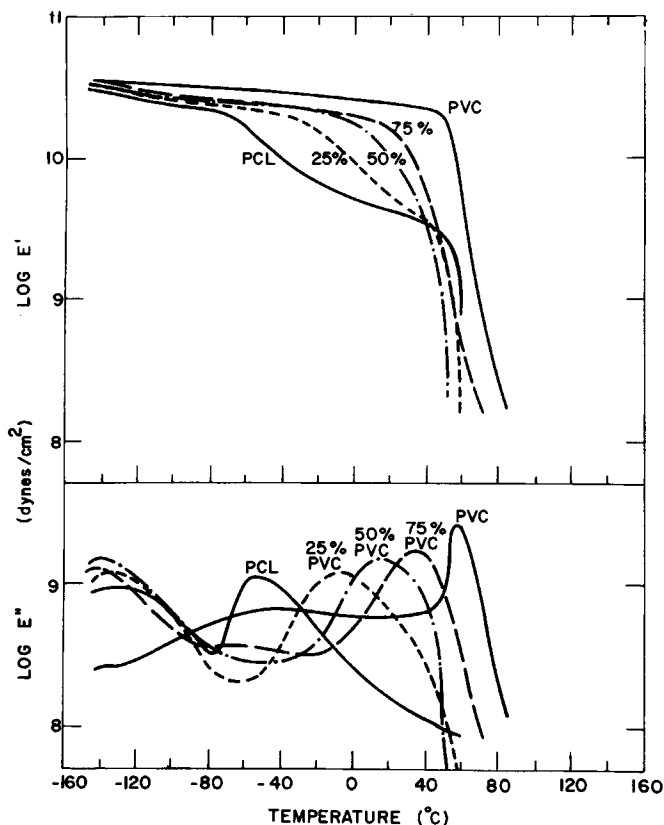


Fig. 5. Temperature dependence of  $E'$  and  $E''$  for PVC/PCL.

## RESULTS AND DISCUSSION

### Thermal Analysis

The DSC glass transitions for each of the three blend systems, PVC/PCL, NC/PCL, and CAB/PCL, are plotted as a function of composition in Figures 1 to 3. These data include the results for samples annealed at room temperature and also for the same samples which have been heated above the melting point of PCL ( $400^\circ\text{K}$  for NC- and PVC-containing samples and  $450^\circ\text{K}$  for CAB mixtures) and then quenched rapidly in the DSC to  $150^\circ\text{K}$ .

In random copolymers, there is a high degree of interaction between the different repeat units because they are held together chemically. The glass transition of a random copolymer consequently reflects the composition of the copolymer. Thus, the  $T_g$  of random copolymers can usually be represented as a monotonic function of composition by one of the various copolymer equations. Similarly, if blends of polymers are mixed at the segmental level, only one  $T_g$  should be evident, and a copolymer equation should be applicable. If a blend system shows only one  $T_g$  for a range of composition but these  $T_g$ 's fail to show a continuous progression from the  $T_g$  of one pure component to the  $T_g$  of the other, the  $T_g$  seen for some of the blends probably represents only one phase in a multiphase system.

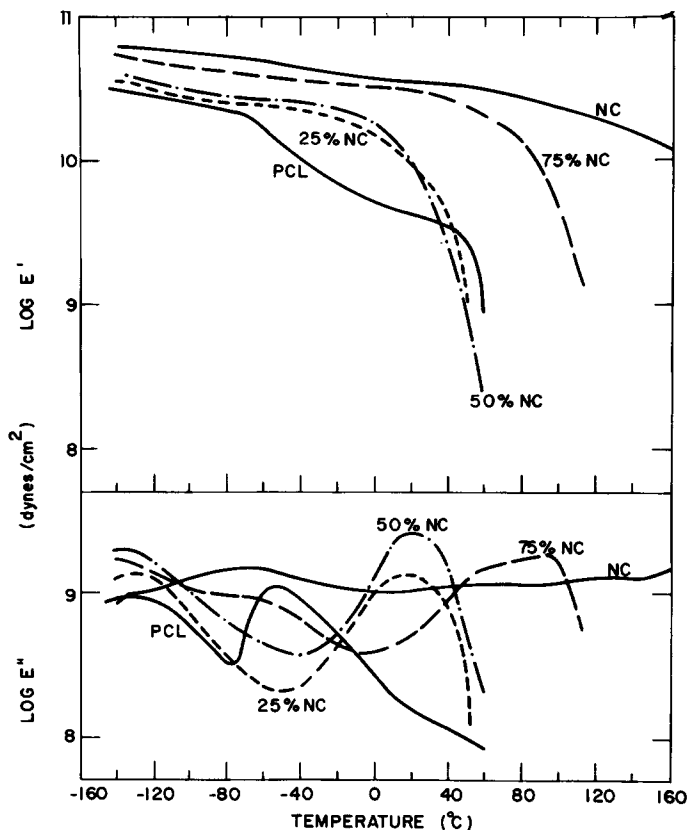


Fig. 6. Temperature dependence of  $E'$  and  $E''$  for NC/PCL.

The Gordon-Taylor copolymer equation, eq. (2), has been applied to the  $T_g$  data in this study to determine if the blends are single-phase systems or not. For a well-mixed system, the plot of  $T_g$  versus  $[(T_{g2} - T_{g12})W_2/W_1]$ , where  $W_1$  and  $W_2$  are the weight fractions of polymers 1 and 2, respectively, in the amorphous phase, will yield a straight line with a slope of  $k$  and an ordinate intercept of  $T_{g1}$ .

The  $T_g$ 's for the PVC/PCL and NC/PCL systems were plotted versus  $[(T_{g2} - T_{g12})W_2/W_1]$  in Figure 4. For the quenched samples,  $W_1$  and  $W_2$  are the weight fraction of PCL and PVC or NC, respectively. Straight lines have been fitted by least-squares analysis to these data. For the unquenched samples,  $W_1$  is the weight fraction of PCL in the amorphous phase. The percent crystallinity of PCL was calculated from the DSC heat of fusion measurements. The variable  $W_2$  is the weight fraction of PVC or NC in the amorphous phase assuming that all of the PVC and NC was noncrystalline.

Figure 1 shows that the Gordon-Taylor equation fits the quenched data for the PVC/PCL blends quite well. The thermograms for the blends of 25%, 35%, and 50% PVC display PCL heats of fusion, and consequently, the unquenched  $T_g$ 's for these samples lie above the curve because the crystallinity reduces the concentration of PCL in the amorphous phase.

The NC/PCL data plotted in Figure 2 present a different situation. Blends

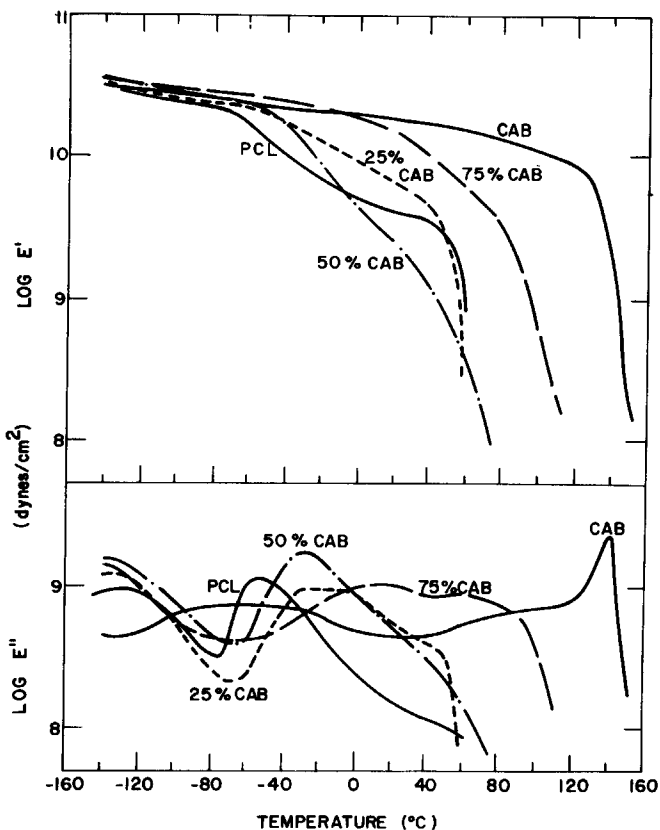


Fig. 7. Temperature dependence of  $E'$  and  $E''$  for CAB/PCL.

of 25% and 40% NC showed the opaqueness and a DSC endotherm which indicate the presence of crystallinity. Consequently, melting and quenching produced lower  $T_g$ 's as expected. Pure nitrocellulose and 50% NC did not show either of these features. Yet, the  $T_g$  dropped from 338° to 328°K for NC and from 283° to 271°K for 50% NC after the heating-quenching cycle. Blends of 65% and 75% NC showed high initial  $T_g$ 's but failed to show any transition after quenching.

The Gordon-Taylor equation fits the quenched points reasonably well for 25%, 40%, and 50% NC. Thus, NC/PCL blends appear to be compatible in the range of 0–50% NC. The unquenched 50% NC does not fit onto the curve even though it did not contain crystalline PCL. Consequently, it would seem that microheterogeneity is present in coarse enough form to allow detection of one of the phases and that the segregation was eliminated by the heating. This trend is continued for 65% and 75% NC. Obviously, large-scale phase separation has produced nearly pure nitrocellulose domains in the 65–75% NC region.

The  $T_g$  data for the CAB/PCL blend system are shown in Figure 3. The thermograms for the samples in the range of 0–50% CAB indicate that PCL crystallinity was present. Above 50% CAB, the samples were clear and exhibited no endothermic heats of fusion in the temperature range tested. Cellulosic derivatives often have some crystallinity. As supplied, CAB showed a small amount of crystallinity which melted at 441°K, but none of the spin-cast films

which contained CAB exhibited this endotherm. The  $T_g$  for pure CAB was measured as 321°K which compares well with a literature value<sup>31</sup> of 323°K; but after heating to 450°K followed by quenching, the thermogram was without transitions.

The quenched  $T_g$ 's in Figure 3 show a steady increase with increasing amounts of CAB up to 60% CAB, after which the  $T_g$  seems to be fairly constant for the 60–85% range. A 91% CAB sample was prepared and tested but showed no transitions. Although the quenched points in the 25–60% CAB range seems to extrapolate to about 200°K, the Gordon–Taylor equation could not fit the data because the Gordon–Taylor plot (not shown) formed a curve rather than a straight line. A Fox equation, eq. (1), curve has been added to Figure 3 as a reference to the expected trend for a compatible system.

A close inspection of Figure 3 shows that for the blends tested, essentially all of the unquenched data and all of the quenched data for samples which were originally noncrystalline fall in the range of 238–248°K, with a somewhat random distribution around an average of 243°K. These results imply that for blends of 25–85% CAB, there are two phases of which one has a fairly constant composition of about 57% CAB judging by the Fox equation. In blends of less than about 50% CAB, the other phase is mostly PCL, and crystallization takes place. Melting followed by quenching forces more PCL into the CAB-rich phase with a lowering of its  $T_g$ . Above 50% CAB, the blend has excess CAB, and this excess forms a second amorphous phase which does not usually show a  $T_g$  in the DSC experiments.

In addition, the heat capacity change associated with the  $T_g$  for samples with more than 50% CAB gets smaller with decreasing concentrations of PCL until it disappears above 85% CAB. Thus, the CAB/PCL blends appear to be only partially compatible. The quenched  $T_g$  of the PCL-rich blends rises with increasing concentrations of CAB but does not follow either the Gordon–Taylor

TABLE II  
Glass Transition and Secondary Relaxations for  
PCL Blend Systems

Blend	Glass transition, °C			Secondary relaxations, °C	
	$\tan \delta$	$E''$	DSC <sup>a</sup>	$\tan \delta$	$E''$
PCL	-41	-56	-63	-125, —	-130, —
25% PVC	8	-4	-33	-132, —	-135, —
50% PVC	50	16	8	-134, —	-132, —
75% PVC	60	36	27	-137, -58	-139, -58
PVC	70	58	83	—, -33	—, -38
25% NC	—	18	-14	-126, —	-130, —
50% NC	—	23	10	-130, —	-138, —
75% NC	52	63, 95	66	-138, -60	-140, -60
NC	88	—	65	—, -60	—, -68
25% CAB	-28, -2	-28, -10	-34	-129, —	-140, —
50% CAB	0	-30	-29	-135, —	-144, —
75% CAB	28	8, 64	-28	-140, —	-140, —
CAB	72	72	48	—, -35	—, -60

<sup>a</sup> The PVC containing samples for the DSC had been annealed and dried at 105°C where as the PVC/PCL samples used in the dynamic mechanical testing had been dried only at room temperature and probably contained a small amount of residual solvent.

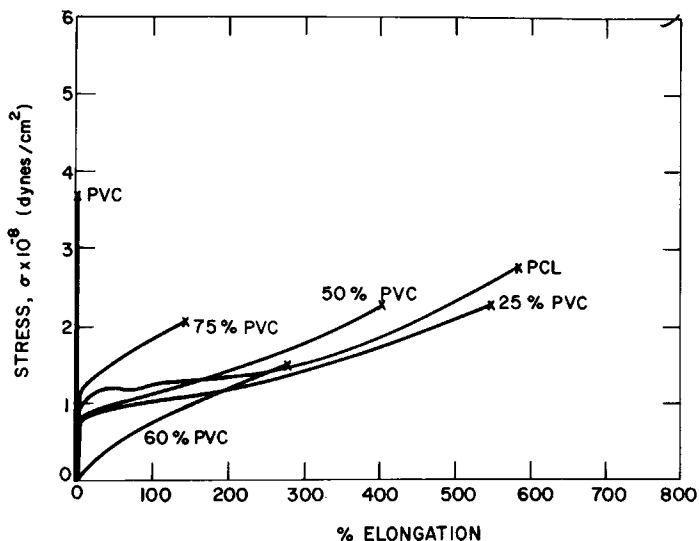


Fig. 8. Stress-strain curves for PVC/PCL at a strain rate of 10%/min. Crosses indicate the points of failure.

or Fox equation. At high CAB concentrations, the apparent  $T_g$  is essentially constant, which implies that a second, CAB-rich phase forms.

### DYNAMIC MECHANICAL TESTING

The dynamic mechanical properties of the PVC/PCL, NC/PCL, and CAB/PCL blend systems are shown in Figures 5 to 7. Peak positions for the  $E''$  and  $\tan \delta$  (not shown) curves are summarized in Table II. Besides the information on the dynamic moduli, these results also give another measure of the glass transition. Although the  $T_g$ 's found by this method are somewhat less precise than those found by the DSC, it has been shown<sup>32,33</sup> that mechanical testing can detect segmental motion on a smaller scale than thermal analysis. Thus, multiple phases may be more easily detected.

In Figure 5, the dynamic mechanical properties for PVC/PCL blends are shown as a function of temperature. Each homopolymer exhibits two relaxations in the  $E''$  curve. The higher temperature peak corresponds to a glass transition, while the lower temperature peak may be attributed to a secondary relaxation.<sup>11,14</sup> In the blends, only one glass transition peak is evident in the  $E''$  curves, though the secondary relaxations of the homopolymers are also evident to some extent. The sharp declines in the  $E'$  and  $E''$  curves for PCL and 25% and 50% PVC in the neighborhood of 50°–60°C can be attributed to the melting of the crystalline PCL.

The dynamic mechanical testing results confirm the compatibility of the PVC/PCL system. At higher concentrations of PVC, the  $\tan \delta$  and  $E''$   $T_g$ 's move progressively to higher temperatures. The symmetry of all the higher temperature peaks implies that they represent single relaxation phenomena.

The secondary relaxation also seems to shift with blending. As Koleske and Lundberg noted,<sup>11</sup> the lower-temperature PCL relaxation at -130°C on the  $E''$  curve can be attributed to movement associated with the  $-(CH_2)_5$  methylene

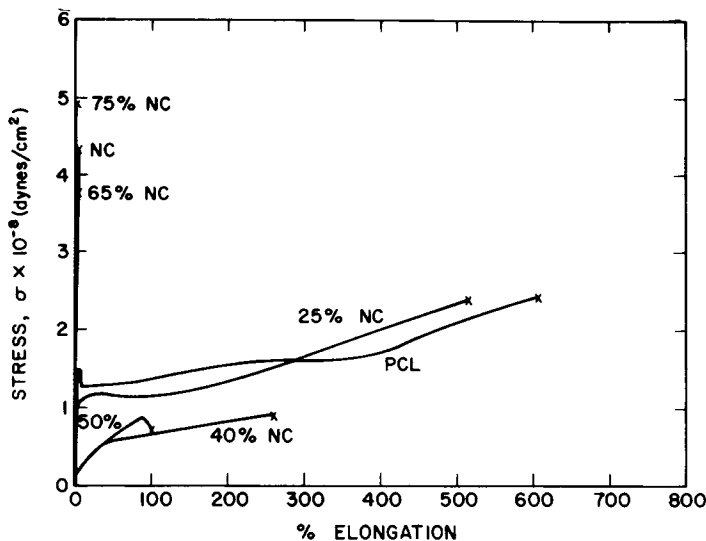


Fig. 9. Stress-strain curves for NC/PCL at a strain rate of 10%/min.

sequence. It has been suggested<sup>34,35</sup> that the movement can be compared to a crankshaft-type rotation around the backbone. As was previously reported,<sup>11</sup> the transition seems to move to lower temperatures upon blending. The broad PVC secondary relaxation at  $-38^{\circ}\text{C}$  on the  $E''$  curve also tends to shift to lower temperatures with blending and disappears at high concentrations of PCL.

The dynamic mechanical testing results for NC/PCL blends are presented in Figure 6. The  $E'$  curves for 25% and 50% NC seem quite similar, with the samples becoming very soft in the region of the PCL melting point. The 75% NC and 100% NC samples maintain high elastic moduli to much higher temperatures. The  $E''$  curves for the blends show the PCL methylene relaxation at lower temperatures and prominent peaks above  $0^{\circ}\text{C}$ . The NC sample seems to lack a relaxation peak which would correspond to a  $T_g$ , but does show a broad peak centered at about  $-68^{\circ}\text{C}$ . This peak also appears to be present in the 50% and 75% NC samples.

The lack of an obvious NC  $T_g$  peak makes analysis of this blend system somewhat ambiguous. The major transition of the 25% NC blend as shown by the  $E''$  curve is the melting of the PCL at  $18^{\circ}\text{C}$ . The  $T_g$  of the amorphous 50% NC blend is in a similar temperature range at  $23^{\circ}\text{C}$ . The symmetry of the  $E''$  peak for the 50% NC blend suggests a compatible blend, since only one relaxation is present.

In the 75% NC blend curve, the interpretation is quite different. The broad relaxation seems to have components at  $63^{\circ}$  and  $95^{\circ}\text{C}$ . Possibly, the upper component of the  $E''$  relaxation represents the  $T_g$  of a nearly pure NC phase. Brode and Koleske<sup>36</sup> measured the NC  $T_g$  at  $115^{\circ}\text{C}$  with a torsion pendulum. The peak at  $63^{\circ}\text{C}$  would then represent a second phase containing both NC and PCL.

The secondary relaxation associated with NC seems to be unaffected by the presence of the PCL in 75% NC. Likewise, in 50% NC, this relaxation, which appears as a shoulder on the lower PCL peak in both the  $E''$  and  $\tan \delta$  curves, seems to be in approximately the same position. This peak can be associated

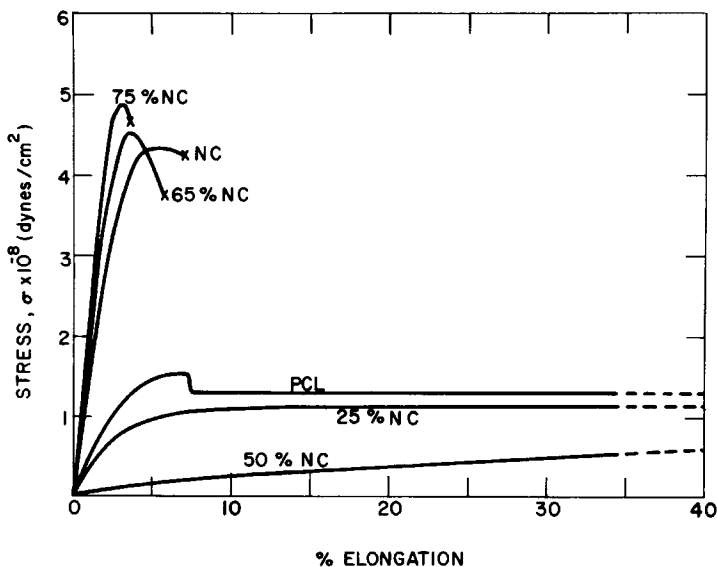


Fig. 10. Stress-strain curves for NC/PCL in the range of 0–40% strain.

with the movement of the six-member anhydroglucose ring.<sup>37</sup> Its low magnitude is most likely due to the steric hindrance caused by the nitro groups which are normally in the equatorial positions. Their bulkiness prevents the ring from switching from one chair conformation to the other.

Like the NC/PCL system, the CAB/PCL dynamic mechanical curves lack the overall symmetry of the compatible PVC/PCL system. Figure 7 shows that blends of 25% and 50% CAB have prominent  $E''$  peaks around  $-20^{\circ}\text{C}$ , and the PCL methylene relaxation, near  $-130^{\circ}\text{C}$ . Pure CAB exhibits very broad, low-magnitude peaks at  $-60^{\circ}\text{C}$  and  $72^{\circ}\text{C}$  and a conspicuous peak at  $136^{\circ}\text{C}$  in the  $E''$  curve. The 75% CAB blend exhibits a subdued methylene relaxation and a very broad, double peak in the  $-20^{\circ}$ – $80^{\circ}\text{C}$  range.

For CAB, the low, broad peak at  $72^{\circ}\text{C}$  has been designated the  $T_g$ . The peak at  $136^{\circ}\text{C}$  on the  $E''$  corresponds to the crystallization and melting of CAB. For the blends, the  $E''$  curves indicate that two  $T_g$ 's are present in each case. In the 25% CAB blend, the peak corresponding to the  $T_g$  seems to be too broad to be a single phenomena. In 50% CAB, the peak at  $-30^{\circ}\text{C}$  seems to have only one component, but it lies at a very low temperature. Possibly a second  $T_g$  is hidden in the long shoulder of the peak. The 75% CAB clearly has two  $T_g$ 's which are  $56^{\circ}\text{C}$  apart. The low-temperature component at  $8^{\circ}\text{C}$  corresponds to the DSC  $T_g$  of  $-28^{\circ}\text{C}$ , and the higher temperature peak corresponds to a phase of nearly pure CAB. This interpretation is in good agreement with the two-phase model based on the DSC results. Thus, CAB/PCL would seem to be a phase-separated system for 25–75% CAB.

## TENSILE PROPERTIES

Typical stress-strain behavior for homopolymers and selected blends in the range of 25–75% PCL are shown in Figures 8 through 11. Figures 8, 9, and 11



show the stress-strain curves to failure, while Figure 10 shows the results of NC/PCL in the range of 0–40% elongation. The stress-strain results are summarized in Table III. The data are averages of three to four runs for ultimate strength, initial (Young's) modulus, and elongation at failure. Stresses have been calculated on the basis of the initial cross-sectional area.

As was described previously, the PVC blends used for the stress-strain tests were made with 1% thermostabilizer and had been dried at 105°C for two days. A pure PCL sample was given the same thermal treatment. Samples dried at room temperature were found to elongate to higher strain levels, but the same trend as a function of composition was evident in the elongation results.

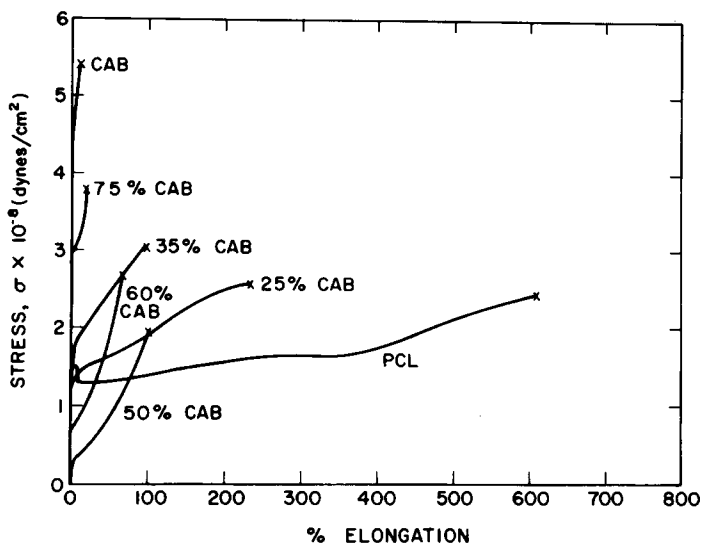


Fig. 11. Stress-strain curves for CAB/PCL at a strain rate of 10%/min.

As Figure 8 and Table III indicate, PCL is a very effective plasticizer for PVC. The ability to elongate rises quickly with higher concentrations of PCL up to about 50% PVC. Simultaneously, the modulus and ultimate strength drop rapidly until 60% PVC. At higher concentrations of PCL, crystallinity is present, and the samples tend to cold draw.

In Figures 9 and 10, it is evident that the NC/PCL blend system exhibits the stress-strain behavior of a system which is compatible over a limited range. The samples in the range of 0–40% NC elongated to over 250%, but the ability to deform drops abruptly between 40% and 65%. The 65% and 75% NC have essentially the same stress-strain behavior as pure NC, which indicates that a nearly pure, continuous NC phase is present.

Figure 11 shows the stress-strain behavior of the CAB/PCL blend system. Although thermal and dynamic mechanical testing showed that, most likely, there is substantial phase separation, the properties shown indicate that PCL is an effective plasticizer for CAB. The modulus drops, and the ability to elongate rises with increasing amounts of PCL. As expected, the modulus drops to a minimum in the sample with the least CAB without having much PCL crystallinity present (50% CAB).

## CRYSTALLINITY STUDIES

*Thermal Analysis*

Bohn<sup>4</sup> in his 1968 survey of compatible polymer blends found that none of the 13 compatible pairs known to him included a polymer capable of crystallizing. He suggested that the exothermic crystallization process was adverse to the mixing process, and, consequently, compatible blends containing crystallinity would be rare. He supported his contention by citing isomeric pairs of polymers which differ only in configuration and the tendency to crystallize but are incompatible. Examples of these include blends of high- and low-density polyethylene<sup>38</sup> and *cis*- and *trans*-1,4-polybutadiene.<sup>39</sup> The following year, Koleske and Lundberg<sup>11</sup> published the first paper on PVC/PCL blends. Since then, the list of crystalline compatible blends has grown to include PVC/Hytrel (a copolyester),<sup>5</sup> poly(vinyl fluoride)/poly(methyl methacrylate),<sup>40</sup> PVC/poly- $\epsilon$ -caprolactam, poly(ethylene terephthalate)/polycarbonate,<sup>2</sup> and all the PCL-compatible blends.

The degree of PCL crystallinity of the blends used in this study has been calculated from the areas under the heat-of-fusion peaks in the DSC thermograms. The results for the PVC, NC, and CAB blends are shown in Figure 12 as percent

TABLE III  
Tensile Properties of PCL Blends

Blend	Elongation, %	Ultimate tensile strength, 10 <sup>-6</sup> dynes/cm <sup>2</sup>	Young's modulus, 10 <sup>-8</sup> dynes/cm <sup>2</sup>
PCL <sup>a</sup>	443	205	29.9
25% PVC	476	202	33.0
50% PVC	383	227	29.0
60% PVC	273	137	1.29
75% PVC	148	210	61.6
PVC	3.1	307	214
PCL	642	264	50.0
25% NC	510	240	38.5
40% NC	285	84.0	6.80
50% NC	104	67.0	4.47
65% NC	5.7	441 <sup>b</sup>	204
75% NC	3.7	497 <sup>b</sup>	243
NC	5.9	414 <sup>b</sup>	270
PCL	642	264	50.0
25% CAB	243	265	56.8
35% CAB	90.6	300	79.4
40% CAB	44.5	206	87.6
45% CAB	37.4	173	53.5
50% CAB	103.	193	8.01
60% CAB	66.5	261	29.0
75% CAB	25.9	392	134
85% CAB	12.7	270	138
CAB	11.2	548	234

<sup>a</sup> Containing 1% PVC thermostabilizer with same thermal history as the PVC containing samples.

<sup>b</sup> Yield points.

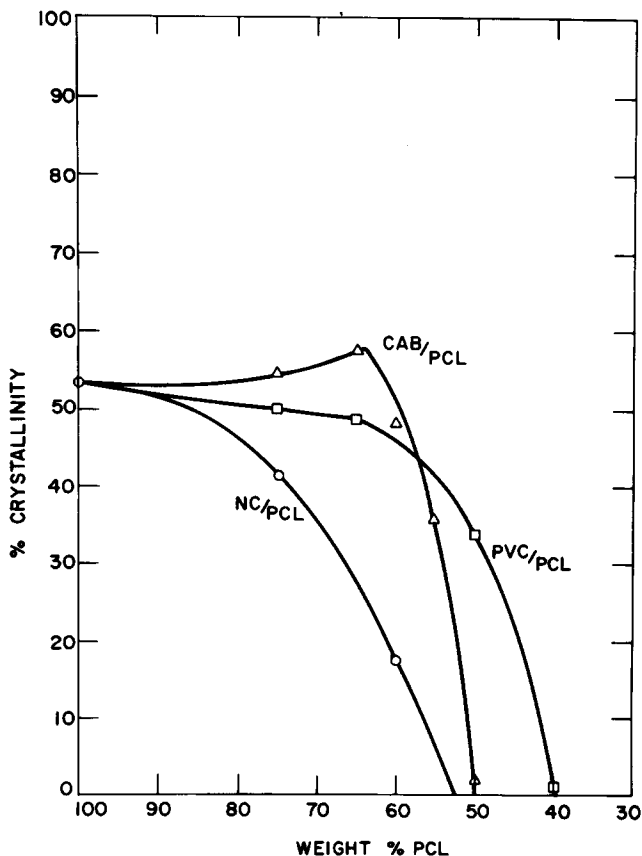


Fig. 12. Degree of PCL crystallinity as a function of composition for PVC/PCL, NC/PCL, and CAB/PCL.

crystalline PCL versus weight percent of the PCL in the blend. Since PCL melts only about 35°C above room temperature, the amount of crystallinity present will increase over a period of weeks or even months with annealing at ambient temperatures. Therefore, data for Figure 12 were obtained from samples which had been aged at least six weeks at room temperature in desiccators.

The data for the PVC/PCL blends are from the samples which were also used for the dynamic mechanical testing. They were aged over four months before the degree of crystallinity was measured. The shape of the PVC/PCL crystallinity curve in Figure 12 is similar to the results of Ong<sup>14</sup> and Khambata,<sup>16</sup> except that they found somewhat higher crystallinities.

The crystallinity data for the nitrocellulose blends were measured for spin-cast films which were used for the stress-strain and dynamic mechanical testing. They were aged six weeks before the DSC work and displayed less crystallinity than the other blends. Possibly over longer periods of time, the crystallinity would rise a few per cent more, but it cannot be expected that the NC/PCL curve on Figure 12 would rise to the levels for the other two blend systems. Even after eight months of aging, a 50% NC sample still did not show a PCL endotherm.

The CAB/PCL blend system differs from the PVC/PCL and NC/PCL systems in the region of high PCL concentration shown in Figure 12 because detectable

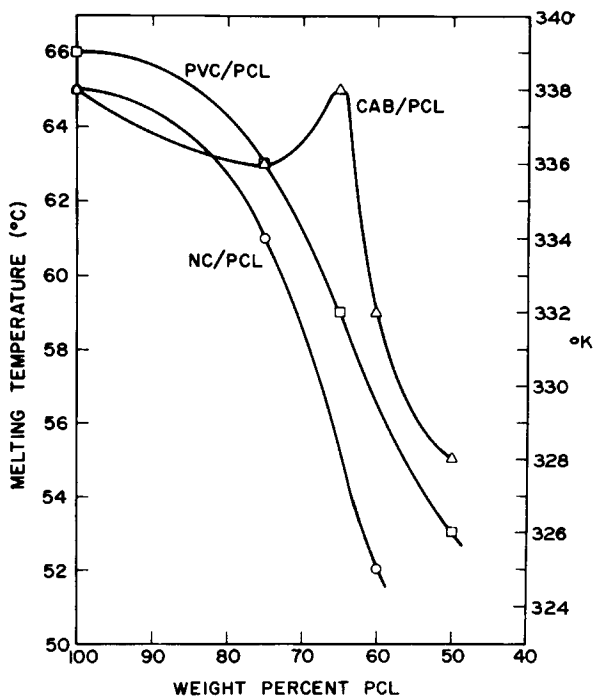


Fig. 13. Melting temperature of PCL as a function of composition for PVC/PCL, NC/PCL, and CAB/PCL.

multiple phases have been shown to be present. The samples which were used for the crystallinity measurements were also used in the stress-strain tests and were aged 11 weeks.

As is seen in Figure 12, there is a noticeable rise in the degree of crystallinity between PCL and 35% CAB, which is followed by a sudden drop to virtually 0% crystallinity at 50% CAB. Lilaonitkul, West, and Cooper<sup>41</sup> have reported that for a phase-separated block copolymer, there is a maximum in crystallinity for one segment as a function of composition which was varied by adjusting the length of the crystallizable segment. They suggested that the amount of crystallinity initially rises with dilution of the crystallizable segment because of incompatibility of the segments and lower viscosity of the system. At higher concentration of the diluting segment, the block lengths of the crystallizable segment become too short for crystallization to take place.

By analogy, incompatibility may enhance the crystallization of a blend component over a limited concentration range. Thus, from 0–35% CAB, incompatibility increases the degree of PCL crystallinity. At higher concentrations of CAB, the constant-composition phase absorbs more of the PCL which would otherwise be in the crystallizable PCL-rich phase. Above 50% CAB, the PCL is drawn into phases with high concentrations of CAB, and crystallization does not take place.

The melting points of the PCL crystalline phase are shown as a function of weight per cent PCL in Figure 13. As PCL is diluted with PVC, NC, and CAB, the DSC melting peak generally shifts to lower temperatures. At the same time, the peak broadens, and the lower temperature tail grows relative to the upper temperature peak.

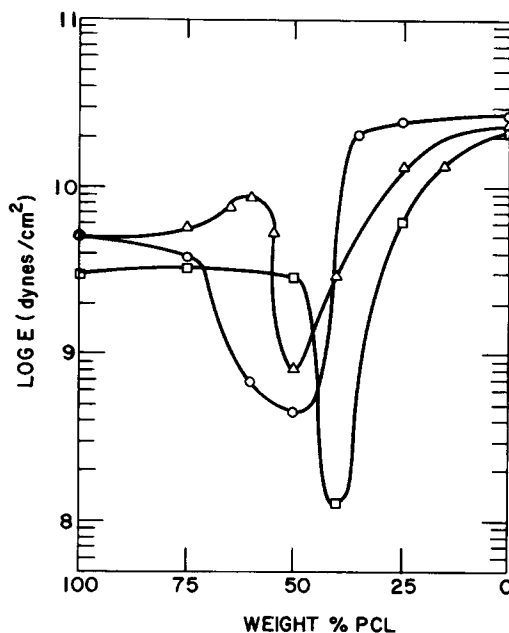


Fig. 14. Young's modulus as a function of composition for ( $\square$ ) PVC/PCL, ( $\circ$ ) NC/PCL, and ( $\Delta$ ) CAB/PCL.

Ong<sup>14</sup> reports that wide-angle x-ray studies show that only one PCL crystalline form is present in all of the crystalline PCL/PVC blends. Thus, he concludes that the drop in melting point  $T_m$  indicates decreasing crystalline order and smaller crystallite size.

After melting and quenching, pure PCL showed no signs of recrystallization upon heating at 20°C/min. Nevertheless, the thermogram showed a smaller amount of crystallinity with a  $T_m$  of 56°C. This PCL crystallinity had crystallized during the quenching process. All blends of 75% PCL and the 65% PCL blends with PVC and CAB showed exothermic recrystallization peaks above their  $T_g$ 's. However, the 40% CAB, 40% NC, and 50% PVC blends failed to reform the PCL crystallinity during the reheating in the DSC. The quenched blends which did show recrystallization all had  $T_m$ 's in the range of 52–54°C.

The rise in the  $T_m$  of the CAB/PCL blends correlates to the rise in the degree of crystallinity discussed previously.

### *Tensile Properties*

The effect of crystallinity on the tensile properties of the blends is shown in Figure 14, where Young's modulus as determined by the initial slope of the stress-strain curves has been plotted versus weight percent PCL. The minimum in the curves for the three systems occurs for samples which were highest in PCL content that could not crystallize. With higher PCL concentrations, the PCL crystallinity increases the modulus of the blends.

The modulus for PVC/PCL blends from 0% to 50% PVC was fairly constant because the decline in crystallinity was slow enough that the increasing concentrations of PVC could compensate for the loss in reinforcement. The PCL sample in the PVC/PCL series had been dried at temperatures above the PCL

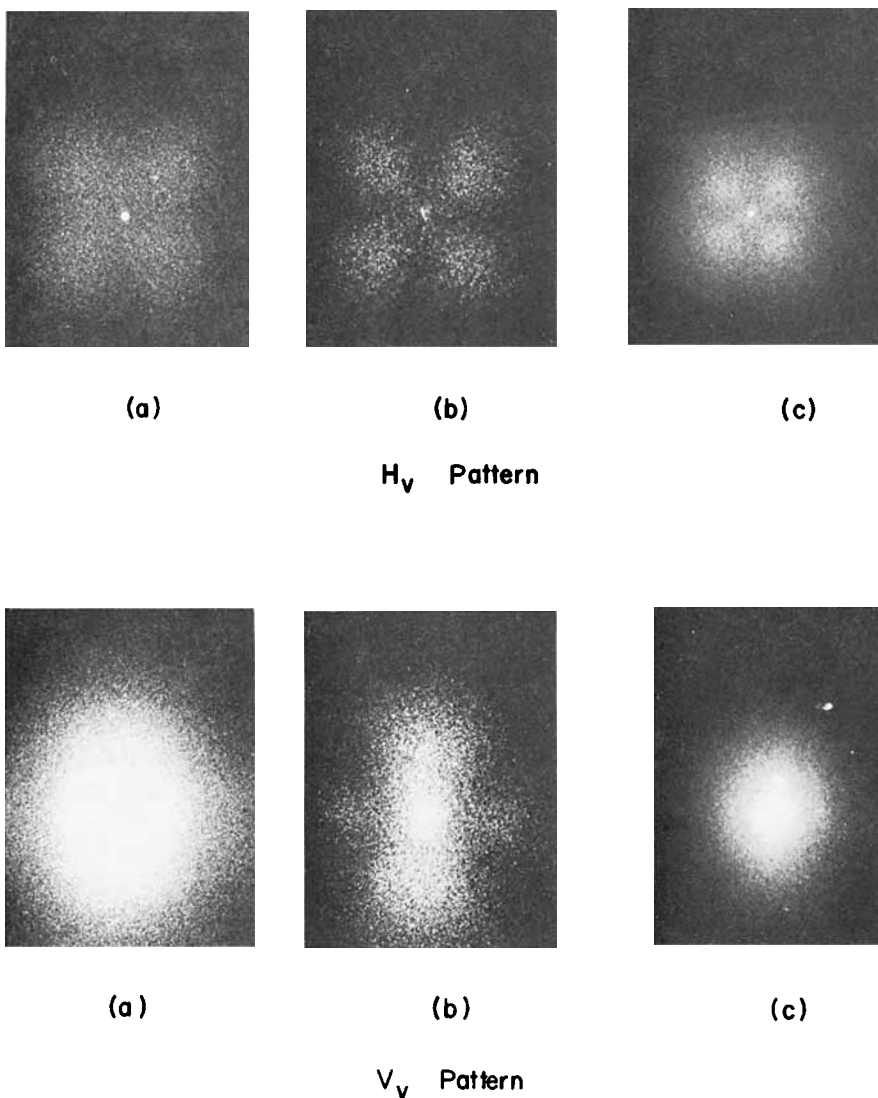


Fig. 15. Small-angle light-scattering patterns for (a) PCL, (b) 25% CAB, and (c) 35% CAB.

$T_m$ , and the crystallinity was about 5% lower than for PCL dried at room temperature. Consequently, the modulus of the pure PCL was lower than the PCL modulus for the two cellulosic blend systems.

In contrast, the degree of crystallinity in the NC/PCL blends drops more rapidly. Thus, the modulus drops off at higher concentrations of PCL. By similar reasoning the rise in modulus in the CAB/PCL blends between 0% and 40% CAB can be attributed to the PCL crystallinity increases in this region.

At low concentrations of PCL, the constancy of the modulus for the NC/PCL system suggests that a continuous phase of NC is present. The rise in the modulus for the other two systems is much more gradual and implies a higher degree of mixing than is evident in the NC/PCL system.

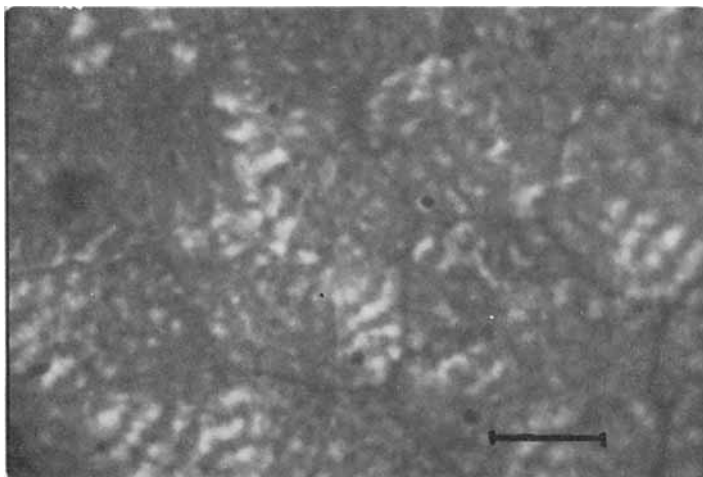


Fig. 16. Cross-polarized light micrographs of 35% PVC. Scale marker is 10  $\mu$ .

### *Morphology Studies*

The  $H_v$  and  $V_v$  scattering patterns for some typical CAB/PCL blends are shown in Figure 15. Similar patterns were obtained with the PVC/PCL system. The scattering patterns show the distinct characteristics for volume-filling negative spherulites. The  $H_v$  patterns display the familiar, well-defined, four-leaf clover design with minimum intensities along the meridian and equatorial axes. This symmetry exists for spherulitic superstructures for the chain axes either perpendicular or parallel to radial direction (negative and positive spherulites, respectively). The  $V_v$  pattern for these blends are also well defined, with scattering present along both axes but with the larger, more intense lobes along the meridian axis. The vertical symmetry identifies these as negative spherulites, and the good resolution is indicative of volume-filling superstructures with a high degree of ordering.

The scattering patterns for PCL and 35% CAB are somewhat less well defined. The PCL and 35% CAB patterns indicate that negative spherulites are present in both, but the lobes of the  $H_v$  patterns are less distinct, and the  $V_v$  patterns are almost symmetric. The lack of sharply defined patterns would imply a high degree of disorder was present. It is also possible that the spherulites are not volume filling.

Nitrocellulose blends (25%, 35%, 40% NC) showed  $H_v$  and  $V_v$  patterns that were essentially radially symmetric (not shown). The maximum intensity was situated in the center of the patterns, and the intensity dropped with increasingly larger scattering angle. These patterns are indicative of randomly distributed crystalline rods which are approximately the size of the wavelength of the laser light.<sup>42</sup>

Ong<sup>14</sup> found that PVC/PCL blends which crystallized from the melt first formed rod-like structures, and then, as the crystallization continued, the scattering patterns of negative spherulites appeared. Furthermore, with SALS and light microscopy, Ong<sup>14</sup> and Khambatta<sup>16</sup> both found that with samples of less than 50% PVC, the PCL crystallinity was volume filling. With 50% or less PCL, regions of pure amorphous material were present.

Since the NC blends showed only rod-like aggregates, it can be inferred that the PCL crystallinity initially goes through the rod-like crystallinity stage. With the PVC and CAB blends, the crystallinity progresses into negative spherulites, but the 25–40% NC blends never get past the initial stage.

The light microscopy studies generally confirmed the SALS studies. Typical cross-polarized micrographs of a 35% PVC blend are shown in Figure 16.

### *Infrared Spectrum Peak-Position Shifts*

If there are acid–base or other attractions between chemical groups on the dissimilar chains, the peak positions of the participating groups should shift to reflect the amount of interaction. In conjunction with infrared dichroism work, the peak positions for the functional groups of the blends of the PVC/PCL and NC/PCL blends were accurately found to the nearest  $0.1\text{ cm}^{-1}$  using a Model 180 Perkin–Elmer IR spectrophotometer with the scales expanded as much as possible. The instrument was calibrated with a polystyrene film.

The  $635\text{ cm}^{-1}$  and  $613\text{ cm}^{-1}$  carbon–chlorine stretching bands of PVC, which represented mostly syndiotactic segments, were found not to shift in blends of 25–91% PVC. Each peak stayed within a  $1\text{ cm}^{-1}$  range and showed no signs of splitting.

The nitrocellulose spectrum exhibits an asymmetric carbon–nitro group stretching peak of  $1659\text{ cm}^{-1}$  which has a shoulder at about  $1652\text{ cm}^{-1}$ . Both constituents stayed within  $1\text{ cm}^{-1}$  of their positions in pure NC for blends as dilute as 24% NC. The only change seemed to be that the lower frequency shoulder decreased somewhat in relative intensity with increasing concentrations of PCL which would indicate that blending reduces the small amount of interaction the nitro groups do have with their environment. The carbon–hydroxyl group at about  $3440\text{ cm}^{-1}$  was much too broad to accurately determine its shift. This peak could also be influenced by the presence of small amounts of water in the sample.

In contrast, the PCL carbonyl showed significant amounts of shifting for both the PVC/PCL and NC/PCL systems, as is seen in Figure 17. The frequency was essentially constant for the 65–100% PCL region for both sets of blends, but rises abruptly where the crystallinity in both systems drops sharply to zero. The effect of the crystallinity is also demonstrated by measuring the carbonyl peak position of crystalline PCL and its melt. In the molten PCL, the carbonyl can be assumed to be unassociated. The carbonyl frequency rose about  $10\text{ cm}^{-1}$  for the following samples when melted:

	C=O frequency, $\text{cm}^{-1}$	
	28°C	75°C
PCL	1725.9	1735.9
25% PVC	1726.3	1734.8
25% NC	1725.7	1735.5

Consequently, the crystalline structure must impose interactions upon the carbonyl.

As the PCL gets further diluted, its frequency tends to decrease. The carbonyl



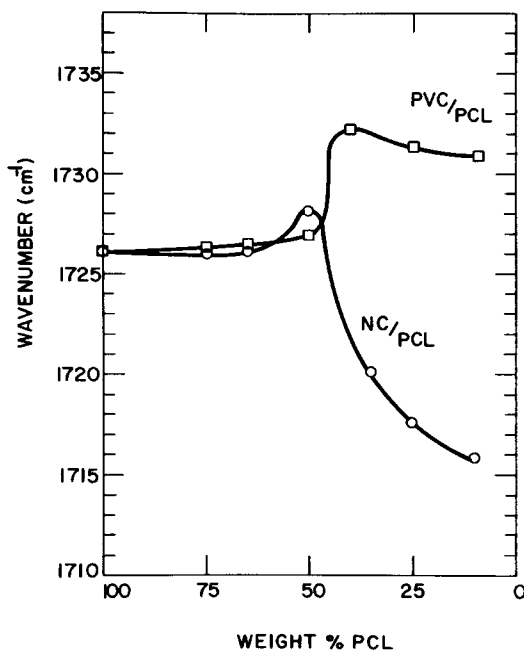


Fig. 17. Carbonyl peak positions as a function of PCL weight percent for PVC/PCL and NC/PCL.

is probably weakly hydrogen bonded to the  $\alpha$ -hydrogen of the PVC, and at very high concentrations of PVC, all of the carbonyls will be bonded. Extrapolating the carbonyl position to 0% PCL, it is found that the frequency of  $1730.6 \text{ cm}^{-1}$  is  $5.3 \text{ cm}^{-1}$  less than for the pure PCL in the molten state.

The decrease in the carbonyl in the NC blends can also be attributed to hydrogen bonding. It has been shown elsewhere<sup>43</sup> that the hydroxyl groups bond to the ester groups of phthalic acid. The effect on the carbonyl is larger due to the stronger nature of the hydrogen bond. The difference in frequency between molten PCL carbonyl and the extrapolated frequency for 0% PCL in a NC blend ( $1715.3 \text{ cm}^{-1}$ ) is  $20.6 \text{ cm}^{-1}$ . The drop in frequency is especially noticeable in the 50–75% NC region where the hydroxyl to carbonyl ratio changes from 0.33 to 0.98. Infrared work was not done with the CAB/PCL blends because the infrared spectra of the two polymers overlap for the bands of interest.

## CONCLUSIONS

Blends of poly- $\epsilon$ -caprolactone (PCL) with poly(vinyl chloride) (PVC) and with several cellulosic derivatives were spin cast from solution. PVC blends with PCL were shown to exhibit only one glass transition temperature ( $T_g$ ), which, for blends quenched from the melt, could be represented as a function of composition by the Gordon-Taylor  $T_g$  equation which is commonly applied to compatible random copolymers.

By a similar criterion, the PCL blends with nitrocellulose (NC) were shown to be compatible for the composition range of 0–50% NC by weight. With higher concentrations of NC, both thermal and mechanical testing indicated that multiple amorphous phases were present, even though the films were clear.

The PCL blends with cellulose acetate butyrate (CAB) were found to exhibit the glass transition behavior of a phase-separated system. Thermal analysis showed that in one phase of the blends, the CAB and PCL were mixed in nearly equal proportions. These conclusions on blend compatibility were generally confirmed by stress-strain measurements for the three blend systems.

The morphology of the PCL crystalline blends was investigated with DSC, small-angle light scattering, and light microscopy. For the PVC blends, PCL crystallinity was found to exist with PVC concentrations as high as 60%. This crystallinity was shown to be in the form of negative spherulites, which were volume filling with up to 35% of the diluting PVC. At higher PVC concentrations, the spherulites decreased in size and were interspersed with amorphous regions.

Stress-strain properties showed a decrease in modulus and increased ductility as the PCL was diluted with the blend polymer. This trend, caused by decreasing PCL crystallinity, is reversed at higher composition levels of the rigid blend component.

The authors wish to thank Dr. J. V. Koleske of the Union Carbide Corporation for supplying samples of polycaprolactone and poly(vinyl chloride). Dr. Robert W. Seymour of the Tennessee Eastman Co. kindly supplied the cellulose acetate butyrate specimen used in this study. Partial support of this research was provided by the Materials and Metallurgy Division of the U.S. Army Research Office and by the donors of the Petroleum Research Fund administered by the American Chemical Society. The authors finally express their appreciation to Mr. Edward M. Sessions who carried out some of the dynamic mechanical testing experiments.

## References

1. F. W. Billmeyer, Jr., *Textbook of Polymer Science*, 2nd ed., Wiley, New York, 1962.
2. R. L. Jalbert, in *Modern Plastics Encyclopedia, 1975-1976*, J. Agranoff, Ed., McGraw-Hill, New York, 1975, p. 107.
3. R. Koningsveld, L. A. Kleintjens, and H. M. Schoffeleers, *Pure Appl. Chem.*, **39**, 1 (1974).
4. L. Bohn, *Rubber Chem. Technol.*, **41**, 495 (1968).
5. T. Nishi, T. K. Kwei, and T. T. Wang, *J. Appl. Phys.*, **46**, 4157 (1975).
6. T. K. Kwei, T. Nishi, and R. F. Roberts, *Macromolecules*, **7**, 667 (1974).
7. J. M. Braun, A. Lavoie, and J. E. Guillet, *Macromolecules*, **8**, 311 (1974).
8. J. V. Koleske, C. J. Whitworth, Jr., and R. D. Lundberg, U.S. Pat. 3,892,821 (July 1, 1975).
9. G. L. Brode and J. V. Koleske, *J. Macromol. Sci.-Chem.*, **A6**, 1109 (1972).
10. C. G. Seefried, Jr., and J. V. Koleske, *J. Macromol. Sci.-Phys.*, **B10**, 579 (1974).
11. J. V. Koleske and R. D. Lundberg, *J. Polym. Sci. A-2*, **7**, 795 (1969).
12. T. G. Fox, *Bull. Am. Phys. Soc.*, **2**, 123 (1956).
13. M. Gordon and J. S. Taylor, *J. Appl. Chem.*, **2**, 493 (1952).
14. C. Ong, Ph.D. Thesis, University of Massachusetts, 1973.
15. F. B. Khambatta and R. S. Stein, *Polym. Prepr.*, **15**, 260 (1974).
16. F. B. Khambatta, F. Warner, T. Russell, and R. S. Stein, *J. Polym. Sci.-Phys.*, **14**, 1391 (1976).
17. G. K. Travis, in *Modern Plastics Encyclopedia, 1975-1976*, J. Agranoff, Ed., McGraw-Hill, New York, 1975, p. 16.
18. D. S. Hubbell and S. L. Cooper, *J. Polym. Sci. A-2*, submitted for publication.
19. O. Olabisi, *Macromolecules*, **8**, 316 (1975).
20. *Hercules Nitrocellulose, Chemical and Physical Properties*, Hercules, Inc., 1969.
21. P. A. Small, *J. Appl. Chem.*, **3**, 71 (1953).
22. K. L. Hoy, *Paint Technol.*, **42**, 76 (1970).
23. J. T. Koberstein, S. L. Cooper, and M. Shen, *Rev. Sci. Instrum.*, **46**, 1639 (1975).
24. J. Malac, V. Altmann, and J. Zelinger, *J. Appl. Polym. Sci.*, **14**, 161 (1973).

25. J. Malac, E. Simunkova, and J. Zelinger, *J. Polym. Sci.*, A-1 (1969).
26. V. Crescenzi, G. Manzini, G. Calzolari, and C. Borri, *Eur. Polym. J.*, **8**, 449 (1972).
27. R. J. Samuels, *J. Polym. Sci. A-2*, **9**, 2165 (1971).
28. R. S. Stein and M. B. Rhodes, *J. Appl. Phys.*, **31**, 1873 (1960).
29. R. S. Stein and P. Wilson, *J. Appl. Phys.*, **33**, 1914 (1962).
30. R. S. Stein, P. Erhardt, J. J. Van Aartsen, S. Clough, and M. Rhodes, *J. Polym. Sci. A-2*, **9**, 295 (1971).
31. W. A. Lee and G. J. Knight, in *Polymer Handbook*, J. Brandrup and E. Immergut, Eds., Wiley-Interscience, New York, 1966, Chap. III, p. 84.
32. J. Stoelting, F. E. Karasz, and W. J. MacKnight, *Polym. Eng. Sci.*, **10**, 133 (1970).
33. W. J. MacKnight, J. Stoelting, and F. E. Karasz, *ACS Adv. Chem. Ser.*, **99**, 29 (1971).
34. T. F. Schatzki, *J. Polym. Sci.*, **57**, 496 (1962).
35. R. F. Boyer, *Rubber Rev.*, **34**, 1303 (1963).
36. A. Nakajima, H. Hamada, and S. Hayashi, *Macromol. Chem.*, **95**, 40 (1966).
37. I. J. Heijboer, *Kolloid-Z.*, **171**, 7 (1960).
38. H. B. Stafford, *J. Appl. Polym. Sci.*, **9**, 729 (1965).
39. Y. Minoura, H. Iino, and T. Tsukasa, *J. Appl. Polym. Sci.*, **9**, 1299 (1965).
40. J. S. Noland, N. Hsu, R. Saxon, and J. M. Schmitt, *ACS Adv. Chem. Ser.*, **99**, 15 (1971).
41. A. Lilaonikul, J. C. West, and S. L. Cooper, *J. Macromol. Sci.-Phys.*, to appear.
42. M. B. Rhodes and R. S. Stein, *J. Polym. Sci. A-2*, **7**, 1939 (1969).
43. B. W. Brodman, M. P. Devine, and M. T. Gurbars, *J. Appl. Polym. Sci.*, **20**, 569 (1976).
44. Union Carbide Bulletin F-42501 *NEW Polycaprolactone Polymers PCL-300 and PCL-700*, 1969.

Received September 20, 1976

Revised November 18, 1976